Possible transmission experiments with low-velocity helium droplets

A. Wynveen, K. A. Lidke, Y. Lutsyshyn, and J. W. Halley
School of Physics and Astronomy, University of Minnesota, Minneapolis, Minnesota 55455, USA
(Received 10 October 2005; revised manuscript received 19 July 2006; published 9 February 2007)

We show that very low velocity droplets can be used to carry out an experiment to test whether condensate mediated transmission processes can occur in a superfluid droplet of ^{4}He. By appropriately choosing the droplet radius and temperature, we can eliminate the competing roton, phonon, and ripplon mediated elastic transmission events. Then a calculation shows that if a few percent or more of the incident atoms experience anomalous condensate mediated transmission, the effects should be detectable in the droplet trajectories. We consider two forms of the experiment, involving a freely falling droplet in ambient vapor in the first instance and an oscillating droplet in a magnetic trap in the second.

DOI: 10.1103/PhysRevB.75.054506 PACS number(s): 67.40.−w

I. INTRODUCTION

The experimental realization[1–3] of Bose-Einstein condensation in alkali vapor has revived interest in the phenomenon and opened exciting new possibilities of a fuller understanding. Earlier experimental studies of Bose condensation were confined to strongly interacting systems, including superfluid ^{4}He. Despite extensive experimental and theoretical effort, a full theoretical description of the experimental phenomena in these strongly interacting systems has proved elusive. In particular, the Bose condensate has been believed to be the fundamental reason for superfluidity in liquid ^{4}He (since London proposed it[4] in 1938) but experimental information on the nature of the condensate is sparse. Only neutron scattering experiments give direct information[5,6] and interpretation of these has proved difficult. In the neutron scattering approach one studies deep inelastic scattering of relatively high energy neutrons. Interpretation requires the impulse approximation, which in turn requires correction to account for final state interactions. The results put limits on the fraction of the total fluid atoms which are in the condensate, assuming that the condensate exists.

Another type of experimental probe of the condensate in superfluid helium was proposed in Refs. 7–9 some time ago. It was suggested that Bose condensation would lead to a form of anomalous transmission of incident helium atoms through the Bose condensed superfluid, because the quantum mechanical amplitudes for absorption and reemission of bosons (say from state λ) from a system in which there are already n_λ bosons present are, respectively, enhanced by factors $\sqrt{n_\lambda+1}$ and $\sqrt{n_\lambda}$. Because of this effect, absorption and reemission of helium atoms will be strongly enhanced. In the strongly interacting case, Bose condensation is described in terms of the one-body density matrix $\rho_1(\vec{r},\vec{r}')$ (Refs. 10–12) which, in a second quantized formulation is expressed as

$$\rho_1(\vec{r},\vec{r}') = \langle \Phi_N | \psi^\dagger(\vec{r}')\psi(\vec{r}) | \Phi_N \rangle \quad (1)$$

for $\vec{r} \neq \vec{r}'$. Φ_N is the N-body ground state of the system and $\psi^\dagger(\vec{r}')$ and $\psi(\vec{r})$, respectively, create a particle at $\vec{r}$ and destroy a particle at $\vec{r}$. The condensate fraction n_0 is defined so that as $|\vec{r}-\vec{r}'| \to \infty$, $\rho_1(\vec{r},\vec{r}') \to n_0 (N/V)$, where V is the volume of the system. The only experimental measurements of the quantity n_0 for superfluid ^{4}He are the deep inelastic neutron scattering experiments mentioned above. The one-body density matrix is the overlap between the wave function $\psi^\dagger(\vec{r}')|\Phi_N\rangle$ with one extra particle at $\vec{r}$ with the wave function $\psi^\dagger(\vec{r})|\Phi_N>$ which is a wave function with one extra particle at a far away point $\vec{r}$. The existence of a condensate fraction means that this overlap remains finite at macroscopic distances so that one may expect amplitudes for processes in which a particle is added at $\vec{r}$ and removed at $\vec{r}'$ will be observable with amplitudes essentially independent of the distance between the two points. We proposed to create an experiment in which particles are added and removed from the fluid in this way in order to probe the structure of the one particle density matrix at large spatial separations directly. In the dilute, effectively weakly interacting system of the condensed alkali gases, calculations exhibiting this effect were carried out for suspended spheres of Bose-Einstein condensed gases[13] and for suspended slabs of such gases.[14]

In strongly interacting helium the proposed condensate mediated transmission can be described as taking place through a virtual quantum mechanical process in which there is quantum mechanically coherent mixing of the state consisting of a free particle and the N particle Bose condensed liquid ground state and a (boosted) state consisting of $N+1$ particles in the Bose condensed liquid ground state. Because these states differ in energy by an energy of the order of the chemical potential of about 7 K, one expects a time delay of the order of $\hbar/7\ \mathrm{K} \approx 10^{-12}$ s for the reemission of the incident atom in such a process. The transmission amplitude and phase for this process were estimated both phenomenologically[7] and variationally[15] and gave amplitudes and transmission times which were consistent with the uncertainty principle estimate. In principle, the amplitude of the condensated mediated transmission, if observed, can provide direct information about the magnitude of the condensate fraction. (The simple relations between this amplitude and the magnitude of the condensate fraction given in Ref. 7 are only valid when the cross-sectional area of the incident wave packet is very small.) In the real system, other processes will compete with this process when a low energy ($\approx$1 K) helium atom is incident on the fluid. These include roton or phonon creation with atomic absorption followed by roton or phonon destruction together with atomic remission, as well as atomic absorption accompanied by creation of one or more ripplons. It

is unclear whether these will swamp the coherent, condensate mediated process and render it unobservable. Some insight into the effects of dissipation was obtained from a recent calculation[13] in weak coupling theory of the scattering of an atomic beam from a weakly interacting Bose condensed spherical sample of atoms of identical type, where negligible dissipative effects were found.

Three versions of the proposed experiment have been carried out: Wyatt and co-workers[16] carried out an experiment on an array of superfluid helium tubes and reported roton mediated atomic transmission. Incident atomic energies were up to 4.5 K above the vacuum level. Lidke and co-workers recently reported an experiment[17] on a film of superfluid suspended in a cesium coated orifice and reported transmission which they attributed to phonon mediated transmission. Neither of these papers reported a prompt signal of the sort expected for condensate mediation. Of the various possible reasons for this, one possibility is that in both experiments, the superfluid sample is strongly coupled to its environment (a tube or an orifice) making the envisioned current carrying boost of the superfluid in the virtual intermediate state difficult to achieve.

A third, experimentally quite different, version of the proposed experiment, carried out by Harms and Toennies[18] has the advantage that this strong coupling to the environment is not present. In this version, energy and momentum transfers from an essentially stationary ^{4}He vapor to moving superfluid ^{4}He droplets was measured. Very interesting effects were seen both for ^{4}He atoms and ^{3}He atoms incident on the droplets, including anomalously *high* energy transfers from ^{4}He atoms to the droplets. However, in the experiments by Harms and Toennies, the lowest internal excitation energy (in the reference frame of the droplet and relative to the ground state energy of the droplet) of ^{4}He atoms entering the droplet was around 12 K (about 5 K relative to vacuum), which is around the "maxon" feature in the helium superfluid excitation spectrum. At such energies, multiple quasiparticle excitation is likely to mask the effects of interest to us. In Toennies' apparatus, it was not possible to carry out the experiment described in Ref. 7 with incident atoms having energies relative to the ground state energy of the droplet as low as 7.5–8.5 K where we expect the quasiparticle effects to be much smaller because rotons cannot be excited with atoms of the average incident energy (Fig. 1). Here we analyze another, distinctly different, way to carry out the experiment on droplets moving through ambient vapor, but at much lower velocities than in the Toennies experiment.

In the version of the experiment proposed in the present paper, droplets move through a stationary vapor, as in the Toennies experiment, but the acceleration of the droplets is provided by gravity, rather than by ejection of gas from a nozzle at high pressures. As a result, the average incident velocities of the vapor atoms on the droplet will be much lower than they were in the Toennies experiment and will excite fewer quasiparticles while the amplitude of the condensate mediated effect is expected to be larger. Our analysis shows that droplets moving at 1 m/s can be produced. We propose to monitor the trajectories of such droplets and to detect the extent to which the droplets are more transparent to the vapor than they would be if the only processes were

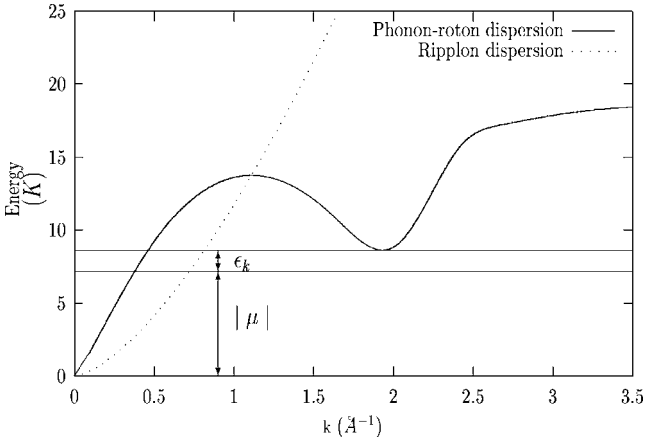

FIG. 1. Energies associated with the processes discussed here. ϵ_k is the kinetic energy of the incident atom (relative to the vacuum level). In the figure, μ is the chemical potential (−7.16 K).

inelastic absorption and emission of atoms and quasiparticle mediated transmission. As discussed, such an experiment will complement the others carried out and under way in two ways: (1) The droplets are falling freely and no mechanical or thermal environment, except for the ambient gas, can interfere with the processes proposed for condensate mediated transmission and (2) very low incident atomic velocities can be achieved. The latter point is important because both variational[15] and weak coupling[13] theoretical studies indicate that condensate mediate transmission amplitudes increase with decreasing incident momentum of the incident atoms on the superfluid. Though the experimental study of such falling droplets poses some experimental challenges which we discuss here, the experiment should be considerably less complicated and difficult than the suspended superfluid experiments which have already been performed. Production of droplets at low velocities has been discussed by the Brown group.[19] We discuss implementation of such an experiment in which droplets are freely falling and in which they are trapped in a magnetic parabolic well in the next section. In the third section we discuss methods for detection of the motion. The paper ends with a discussion and conclusions.

II. ANALYSIS

We first envision introducing one or more droplets into a cryostat and watching the droplet fall freely in the gravitational field. (The gravitational acceleration is g. We choose a z axis pointing downward in the ensuing equations.) The processes by which atoms of the vapor might affect the trajectory of the droplet are of four types: (1) Absorption of atoms of the vapor into the droplet inelastically with no immediate or coherent reemission. (2) Emission of atoms from the vapor not coherently related to any previous absorption; (3) absorption of atoms of the vapor with production of a quasiparticle (roton or phonon) which propagates across the droplet and is annihilated elastically with the emission of an atom at another place on the surface of the droplet [a related possibility is the excitation of one or more ripplons during atomic absorption followed by reemission of an atom after

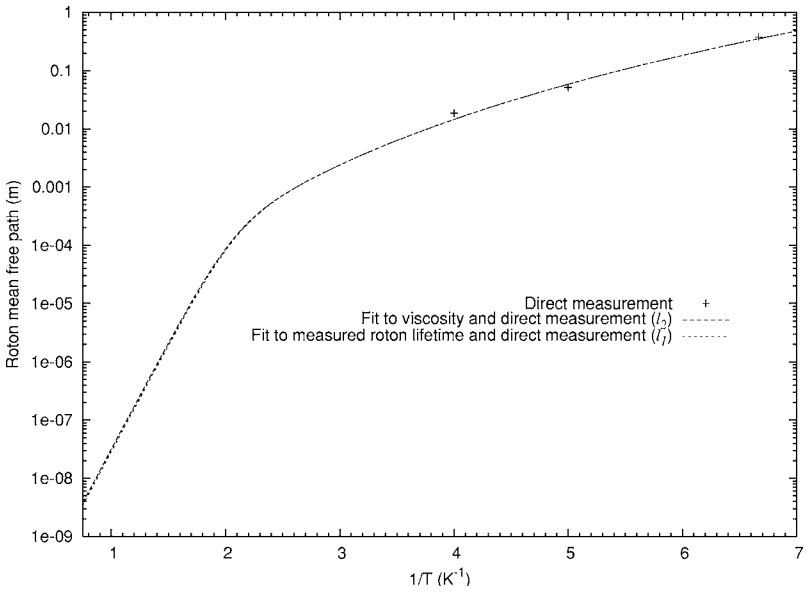

FIG. 2. Interpolation of roton mean free paths between measured values from 0.15 K to 0.25 K and two estimates (visually almost indistinguishable on this logarithmic scale) for the mean free path at temperatures around 1 K as discussed in the text.

the ripplon(s) have propagated to the opposite side of the droplet[20]]; and possibly, (4) condensate mediated transmission of atoms of the vapor through the droplet elastically. We will argue that, by appropriate choice of droplet size and temperature, the processes of type (3) can be made insignificant, so that we have only inelastic processes (1) and (2) and, if it exists, type (4) elastic transmission. We then make an analytical calculation of the effects of processes of types (1) and (2) on the trajectory and argue that experimental deviation of the trajectory from the prediction is evidence of processes of type (4).

In such an experiment, the mean velocities of helium atoms incident on the droplet range from 0 at the beginning of the trajectory to <1.5 m/s at the end (assuming a distance of 10 cm). We wish to design the experiment so that a negligible number of quasiparticles excited by collisions with atoms of the vapor pass through the droplet and elastically cause reemission of atoms. (Such quasiparticle mediated transmission effects can affect the direction of the droplet's momentum but because they are entirely elastic, they cannot affect the average downward velocity of the atom.)

The mean free paths of phonons and rotons were measured directly in the temperature range 0.15 to 0.25 K by the Wyatt group.[21–23] At these low temperatures, their experimental results fit the expression

$$l_{\text{wyatt}} = 0.00025/T^{6.25}\ (\text{cm}). \tag{2}$$

For higher temperatures we did not find any direct measurements. Roton lifetimes have been measured quite precisely in the range 0.8 K to 1.3 K using neutron scattering.[24] The neutron scattering experiments were shown to be in good agreement with the expression

$$\Gamma = 4.052\sqrt{T}\exp(-\Delta/k_B T) \tag{3}$$

for the width of the roton line in meV. We estimate a mean free path from this as

$$l_{\text{neutron}} = \hbar v_r/\Gamma \tag{4}$$

using the expression $v_r=(2k_BT/\pi\mu_r)^{1/2}$ for the mean roton velocity. Here $\mu_r=0.26m_{\text{He}}$ is the effective roton mass. Simply extrapolating this result to low temperatures yields a mean free path which is much higher in the range 0.15 K to 0.25 K than that measured by the Wyatt group. We can interpolate between the two temperature ranges with the expression

$$l_1 = 1/(1/l_{\text{wyatt}} + 1/l_{\text{neutron}}) \tag{5}$$

with the result shown in the curve labelled fit to measured roton lifetime and direct measurement in Fig. 2. By combining calculational results of Landau and Khaltnikov[26] of phonon mean free paths with measured viscosities, Atkins[25] obtained an expression for the mean free path of rotons around 1 K. Atkins expression was

$$l_{\text{atkins}} = 10\eta_r/(\pi v_r \rho_r). \tag{6}$$

Atkins used the value $\eta_r=11.5\times10^{-7}$ poiseuille (assumed temperature independent). v_r is defined as above and ρ_r, the effective mass density of rotons, was taken as

$$\rho_r = \frac{2\mu_r^{1/2}p_0^4}{3(2\pi)^{3/2}(k_BT)^{1/2}\hbar^3}\exp(-\Delta/k_BT), \tag{7}$$

where p_0 is the $\hbar$ times the roton wave vector at the roton quasiparticle minimum. Again, this expression gave much too high a mean free path compared to experiments when extrapolated to the range of the Wyatt measurements. (It was shown in Refs. 21–23 that the basic theoretical approach in Ref. 26 accounts for the low temperature results by going to higher order in perturbation theory.) We interpolate between the low temperature results and the expression given by Atkins with the relation

$$l_2 = 1/(1/l_{\text{wyatt}} + 1/l_{\text{atkins}}) \tag{8}$$

which is also plotted in Fig. 2 with the label fit to viscosity and direct measurement. From Fig. 2, one sees that the two

estimates of the roton mean free path agree in order of magnitude in the region near 1 K where we propose a falling droplet experiment. The roton mean free path is estimated in both cases to be much less than a micron in that temperature region. To ensure that all quasiparticle producing collisions are essentially inelastic in the sense of processes (1) and (2) described above, the droplet sizes must be larger than the roton mean free path.

The remaining mode of quasiparticle production by incident atoms is ripplon creation. An elastic process has been suggested in which a ripplon created by an incident atom propagates around the surface of a droplet and causes elastic reemission of an atom on the opposite side of the droplet.[20] We are not aware of any detailed calculational studies of this possibility. However, it will be irrelevant if the ripplon lifetime is shorter than the time required for the ripplon to propagate around the droplet. For a process in which one ripplon is created by the incident atom (Fig. 1), the highest energy ripplons, arising from incident atoms with energy of the order of 1 K relative to the vacuum, will have an energy of about 8 K above the helium ground state. This corresponds to a ripplon frequency of 10^{12} Hz and a wave number of 10^{10} m^{-1}. We estimated the lifetime of such ripplons using the data in Refs. 27 and 28. At 1 K, we find a damping time for ripplons of energy of 8 K of about 10^{-10} seconds which corresponds to a damping length (damping time multiplied by the velocity of a ripplon at this energy) of 0.01 microns whereas at 0.25 K the expected mean free path, scaling roughly as T^4 will be around 0.03 cm. Thus if the diameters of the droplets are, respectively, greater than a few microns at 1 K (which is consistent with the constraints found above for assuring that roton and phonon creation result in elastic processes) then the ripplon would be damped long before it had time to propagate around the droplet. Similar results were found for a 2 ripplon process in which each ripplon has an energy of 4 K. The damping time is slightly larger than that of the one ripplon process, but the damping lengths are nearly equal since the velocity for these ripplons is lower. These estimates are subject to substantial uncertainty because the temperatures fall in a region in which there appear to be substantial discrepancies between the observed damping rates and the theory proposed in Ref. 27. Furthermore, we have made no attempt to estimate the effects of the finite curvature of the droplet surface on the ripplon damping rates, though we would expect these to be substantial. Despite these caveats, these estimates suggest that an elastic atom-ripplon-atom elastic absorption and reemission process is unlikely under the conditions which we envision for an experiment.

These arguments do not address the possible role of thermally excited ripplons present in local thermal equilibrium on the surface of the droplet. Interactions of incoming atoms with such ripplons will lead to incoherent processes of types (1) or (2) by the same lifetime arguments above. [The role of interactions of thermally excited ripplons with incoming atoms in determining the ratio of the rates of processes of types (1) and (2) to the rate of possible processes of type (4) has not been thoroughly explored. It is not directly relevant to the theme of this paper, which focuses on detecting processes of type (4) experimentally. However one may make the following rough argument: In the experimental conditions envisioned, the incoming atoms will be in wave packets of cross-sectional area of order $(0.5\ \text{nm})^2$ (from the thermal wavelength) and the estimated surface density of ripplons at 1 K is of order 10^{15} m^{-2}. By a simple kinetic argument, an incoming atom will encounter a thermally excited ripplon once in about 5000 atom-droplet collisions.]

From the foregoing arguments we find that if the droplet radius is judiciously chosen, then all collisions of atoms from the vapor will result in inelastic absorption or emission [processes (1) or (2)] unless processes of type (4) (condensate mediation) occur. Let f_i be the fraction of incident atoms inelastically adsorbed and f_x be the fraction anomalously transmitted. These arguments imply $f_x = 1.0 - f_i$ if the temperatures and droplet diameters are chosen in the indicated ranges.

We now calculate the trajectory of the droplet, assuming that a fraction f_i of the atoms absorbed as well as f_i of the atoms emitted from the droplet arise from incoherent inelastic events of types (1) and (2). In this calculation, we obtain an equation of motion for the drop in which a Stokes drag force causes the drop to reach a terminal velocity which inversely depends on the fractional density of the vapor (f_i) which interacts inelastically with the droplet. We assume that the atoms which are effectively transmitted by condensate mediation have no effect on the droplet trajectory. (The matrix elements associated with the virtual mixing process envisioned[7,15] will conserve momentum in a translationally invariant system.)

The resulting equation is similar to that of a sphere moving through a viscous fluid but differs slightly in this situation where atoms are either adsorbed or emitted at the droplet's surface.

The calculation of the momentum transfer to the drop involves studying the contributions to the net momentum flux of adsorbed and evaporated atoms,

$$\frac{d\vec{p}}{dt} = \int\int [\hat{n}\cdot(\vec{v} - u\hat{z})](m\vec{v})\rho(\vec{v})d\vec{v}dS - \int\int (\hat{n}\cdot\vec{v}')[m(\vec{v}' + u\hat{z})]\rho(\vec{v}')d\vec{v}'dS + Mg\hat{z}, \quad (9)$$

where $\hat{n}$ is the unit vector normal to the drop's surface, $\vec{v}$ is the velocity of an absorbed vapor atom, u is the velocity of the drop in the downward direction, $\vec{v}'$ is the velocity of an atom emitted from the drop in the drop's rest frame, M is the mass of the drop, and g is the acceleration due to gravity ($9.8\ \text{m/s}^2$). The integrals are evaluated over the thermal velocity distribution, $\rho(\vec{v})$, of atoms in an ideal gas, and the flux is summed over the surface of the drop, assumed spherical. In solving this equation, we assumed that the mass and temperature of the drop remain unchanged. We show that this assumption is correct to lowest order in u and within our other approximations in the Appendix A. We also assumed that we can neglect the formation of a wake behind the droplet as it falls because the thermal velocities of the atoms in the vapor are much larger than the terminal velocity of the droplet, and the mean free path of the atoms in the vapor is

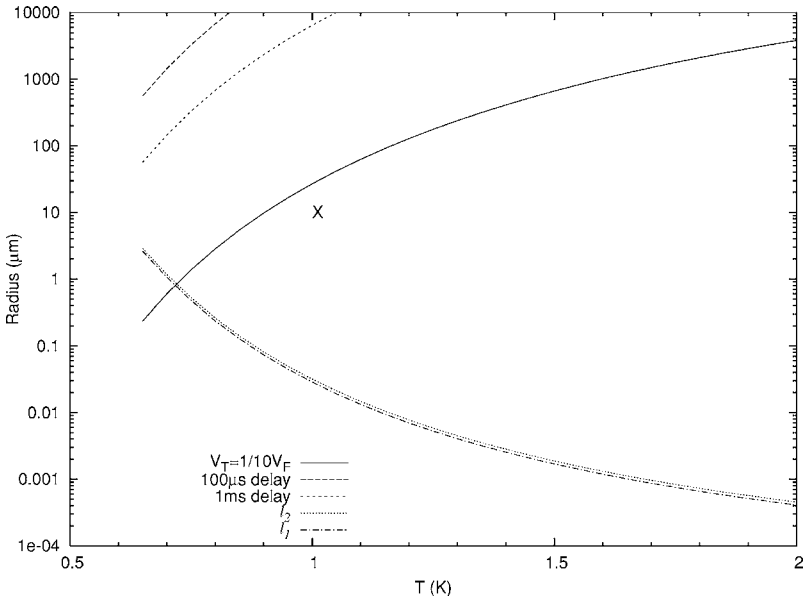

FIG. 3. Constraints on droplet radius and temperature. The first curve gives a maximum R to give a droplet terminal velocity which is a tenth of the free fall velocity at the end of the fall. The second curve gives a maximum R for which the time delay (relative to free fall time) is 100 μs. The third curve gives a maximum R for which the time delay (relative to free fall time) is 1 ms. The fourth and fifth curves give the two estimates of the roton mean free path (corresponding to Fig. 2 and the accompanying discussion). The large $\times$ is in the region in which all the criteria are satisfied.

of the same order as the droplet's radius. The droplet sizes we propose for the experiment are far above the nucleation threshold which we estimate from the requirement $R > (3\sigma)/(\rho_l k_B |\mu|) \approx 5$ Å at 1 K, with the surface tension $\sigma = 3.75 \times 10^{-1}$ erg/cm^2, $\rho_l = 2.1834 \times 10^{22}$ cm^3 and chemical potential $\mu = -7.15$ K.

Evaluating the integrals in (9) by expanding the thermal velocity distribution to first order in $\vec{u}$ after making a change of variables $\vec{v}'' = \vec{v} - u\hat{z}$ in the first integral, we find

$$\frac{dp_z}{dt} = -f_i \frac{4}{3}\pi R^2 u \rho_g \sqrt{\frac{2mk_BT}{\pi}} + Mg, \tag{10}$$

where R is the radius of the drop, ρ_g is the number density of the vapor, m is the mass of a helium atom, k_B is Boltzmann's constant, and T is the temperature of the vapor and the droplet. This yields a terminal velocity of

$$u_T = \frac{\rho_l}{\rho_g} mgR \sqrt{\frac{\pi}{2mk_BT}} \Big/ f_i, \tag{11}$$

where ρ_l is the number density of liquid helium. If (see Appendix A) we assume M is constant, then the left-hand side of (10) is Mdu/dt and we can solve the equation exactly for u and hence for z to obtain trajectories, assuming (Appendix A) that the temperature of the droplet is also constant. The solution is

$$z = (g/(\gamma)^2)[\exp(-\gamma t) - 1] + gt/\gamma \tag{12}$$

in which $\gamma = f_i(\rho_g/\rho_l)(1/R)\sqrt{\frac{2k_BT}{m\pi}}$. Notice that γ decreases with increasing droplet radius R because the mass of the droplet increases more rapidly with droplet radius than its surface area. This will lead to the conclusion (see below) that rather small droplets are to be preferred for the experiment. By comparing these results with the observed trajectories we wish to extract a value for f_i and hence information about the transmission coefficient for incident atoms through the droplet. In Appendix B we display how f_i will depend on a transmission coefficient $T(\vec{v})$ which depends on the magnitude and direction of atoms incident on the surface of the droplet. This dependence will lead to a temperature dependence of f_i which might in principle be used to extract experimental information about the function $T(\vec{v})$.

To determine optimal conditions of temperature and droplet size we may consider Eq. (11). Small terminal velocities, on which the quantity f_i, which we wish to measure, depends will be easier to detect than large ones. To get a quantitative idea of the requirements, we suppose that the terminal velocity u_T of Eq. (11) is 1/10 of the velocity $\sqrt{2gd}$ which the droplet would have after freely falling a distance $d = 10$ cm. Then the effects of collisions of the vapor with the droplet on the trajectory will be easily detectable and increases in u_T due to anomalous transmission should also be detectable. We solve the equation $10u_T = \sqrt{2gd}$ (with $f_i = 1$) for R and, using the known values of the saturated vapor pressure (converted to density ρ_g using the ideal gas law) at various temperatures,[29] we plot the result as a function of temperature in Fig. 3. The droplet radius R must lie below this curve in order to satisfy $10u_T < \sqrt{2gd}$ with $f_i = 1$.

If the product of the time and the damping constant γt remain small during the fall, then we can obtain another, less stringent condition on the radius. Expanding the expression for z in powers of γt and assuming that the droplet falls a distance d (for which we take 10 cm in numerical examples) we find that the difference $\Delta t = t - \sqrt{2d/g}$ between the drop time and the free fall drop time is given to lowest order by $\Delta t = (1/3)\gamma d/g$. If we suppose that we can experimentally resolve a value of Δt of order 100 microseconds, then this relation can be solved for R to find another limit on the value of R for which effects of the vapor-droplet collisions can be observed. This limit is also plotted in Fig. 3. This is a much weaker limit, and can be regarded as giving the largest value of R for which any information at all can be extracted about the vapor-droplet collisions. We also plot our estimates of the roton mfp from Fig. 2 in Fig. 3. R must lie above the mean free path curve. One sees that, consistent with keeping the temperature as low as possible, the experiment should be done in a fairly narrow window for which R is below 10 μm

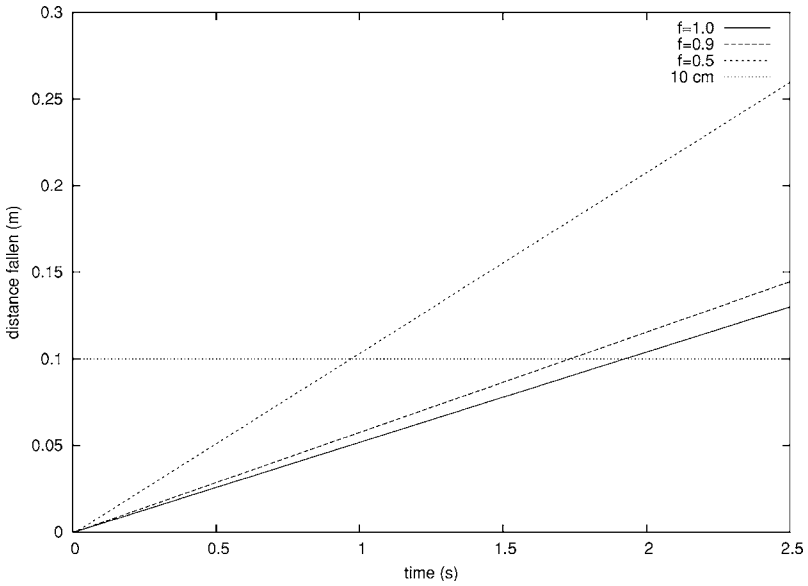

FIG. 4. Trajectories of drops for 10 μm droplets with f_i=1.0, 0.9, and 0.5 at temperature 1.00 K.

and the temperature is between 1 and 1.25 K.

In Fig. 4, we show a few calculated trajectories of a falling drop for different values of f_i, the fraction of incident atoms that are inelastically adsorbed rather than transmitted, for a 1.00 K ambient vapor and a 10 μm radius droplet. If the droplet radius were known exactly (see below) then an easily achievable time resolution of a millisecond would make it possible to distinguish f=0.9 from f=1.0 at the end of a 10 cm fall (horizontal line). To see the effects of an error in the measurement of the droplet radius we compare the trajectories for 10 μm and 11 μm droplets under the same conditions in Fig. 5. Since, as we discuss below, the droplet radius may only be measurable for this size droplet to about ± 10% this figure illustrates the main uncertainty in extracting a value of f_i from the data. If the droplet radius is not measured to better than 10% (which may be possible, see below) then it will not be possible to distinguish data from the cases f_i=1, R=11 μm and f_i=0.9, R=10 μm, for example. In Fig. 6, we show the same information for a 100 μm droplet. From these data it is apparent that a value f_i=0.9 (corresponding to 10% anomalous transmission) could still be detected with a 100 μm droplet and a time resolution of a millisecond.

The Brown group[19] has reported levitation of helium droplets in a magnetic well. In such a well, which is approximately parabolic near its minimum, one can study oscillatory behavior of a droplet. Using the same model described in the preceding paragraph, the equation of motion for an oscillating droplet, along one direction, would be

$$\frac{dv_x}{dt} = -\omega^2 x - \frac{\rho_g}{\rho_l m R}\sqrt{\frac{2mk_BT}{\pi}}v_x, \tag{13}$$

where ω is the angular oscillator frequency of the well (independent of droplet mass). The solutions to this equation are just those of a damped harmonic oscillator. For a 1 μm droplet, the oscillation is overdamped. For larger droplets, the system is underdamped, and the oscillations of the drop-

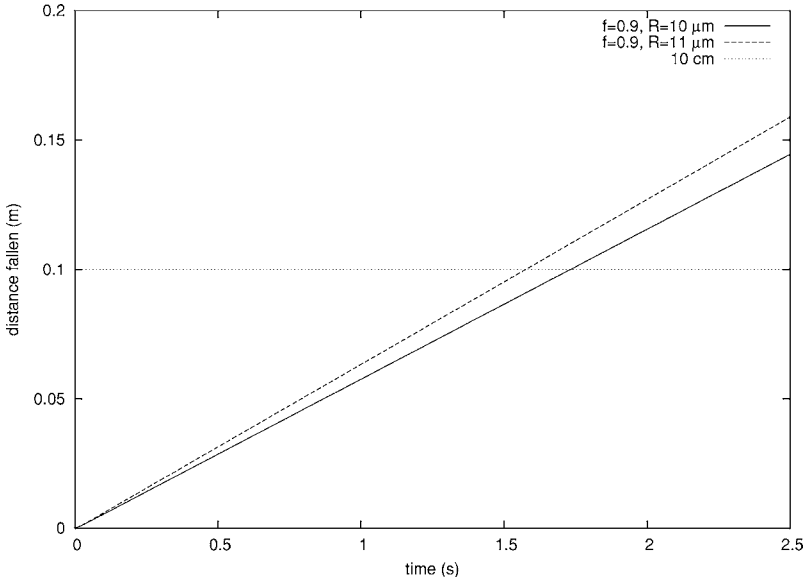

FIG. 5. Trajectories for 10 μm and 11 μm droplets with f_i=0.9 at temperature 1.00 K.

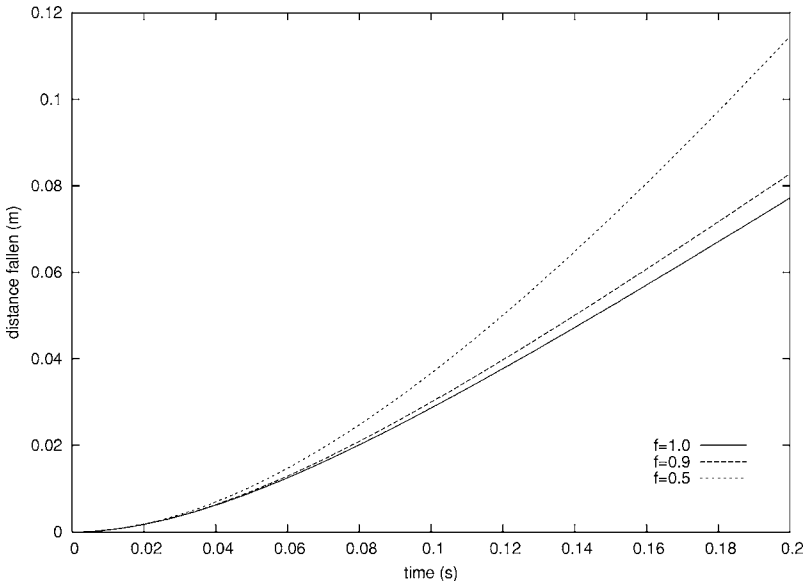

FIG. 6. Trajectories of drops for 100 μm droplets with f_i=1.0, 0.9, and 0.5 at temperature 1.00 K.

let decay at a rate which depends once again on the absorption fraction.

III. PRODUCTION AND DETECTION

Methods for production of droplets have been reviewed by Northby.[30] The most promising method for producing the desired 10 μm droplets is the use of a piezoelectric drive under a superfluid film.[31,32] Both of the cited papers reported production of low velocity 10 μm droplets using this method. In the experiments reported in these papers, the droplets were studied while optically trapped[32] or while moving upward.[31] Consider placing a large diameter tube vertically through the bath in which the piezoelectric which produces the droplet cloud is embedded. Some of the produced drops will fall back down through this tube, providing a source of droplets suitable for the proposed experiment. The vertical velocity of the drops produced was controlled with the voltage on the piezoelectric in the experiment reported in Ref. 31. By adjusting the voltage, the initial upward velocity could be made as low as a threshold value of 36 cm/s. Tuning the voltage to produce drops with initial upward velocity of 40 cm/s, one easily estimates that with an initial upward velocity of 40 cm/s the droplets will start moving downward about 40 milliseconds after they are produced, when they are approximately 0.8 cm from the surface of the liquid in which the piezoelectric device is embedded. The cloud of droplets is reported[33] to spread beyond the surface on which they are produced and to fill the chamber above the liquid vapor interface after the piezoelectric device is pulsed. It would not be difficult to give this chamber sufficient vertical height to allow the drops to rise to the top of their trajectories and begin to fall. Some of those with small initial horizontal components of velocity would then pass through a vertical tube placed in the bath and terminating below the can containing the source liquid and piezoelectric. (Superfluid would slowly siphon from this upper can through a film on the vertical tube. Using the well known properties of such films[34] and assuming that the tube extends 2 cm above the surface of the fluid in an upper can of diameter 2 cm, we estimate a flow rate of about 10^{-3} liters/h out of the upper can. This could be easily replenished during an experiment.) The experiment discussed in this paper would be carried out below this upper can, as falling droplets emerged from the bottom end of the tube. For such a scenario to work, the initial horizontal droplet velocity must be small enough so that the droplet does not strike the side of the tube or of the chamber below the source during the trajectory. For example, droplets produced within 0.1 cm of the tube opening would pass through if they had initial horizontal velocities of 4 cm/s and would move a few centimeters horizontally during their descent. Though the detailed design of a source using this approach has not been carried out, these parameters suggest that it should be possible.

In order to determine a droplet's radius and trajectory, various approaches may be used. In a cryostat with an optical window, the simplest of these might be to periodically photograph the droplet during its fall, using stroboscopically pulsing light or its equivalent. Niemela, in his experiments on levitated charged drops,[35] was able to photograph a falling drop's trajectory using stroboscopic techniques. The Brown group, in their experiments on laser levitation of helium,[32] was able to image micron-sized droplets optically via laser reflection from the droplet surfaces. The motion of a drop could also be determined using techniques similar to those of Bennett *et al.* in their experiments studying bubble entrainment caused by the impact of helium drops on a helium surface.[36] A tilted infrared beam from an IR emitter, which could be reflected and refocused a number of times in order to crisscross the length of the droplet's path, would be defocused by a droplet intercepting the beam. The detected beam could then be used to establish the time dependence of the droplet's motion.

Another possibility is to illuminate the path to be followed by the falling droplets from below with a laser beam, using an optical feedthrough.[38] The droplets will be larger than the wavelength of easily accessible laser light so a geometrical optics interpretation of the light scattering is appro-

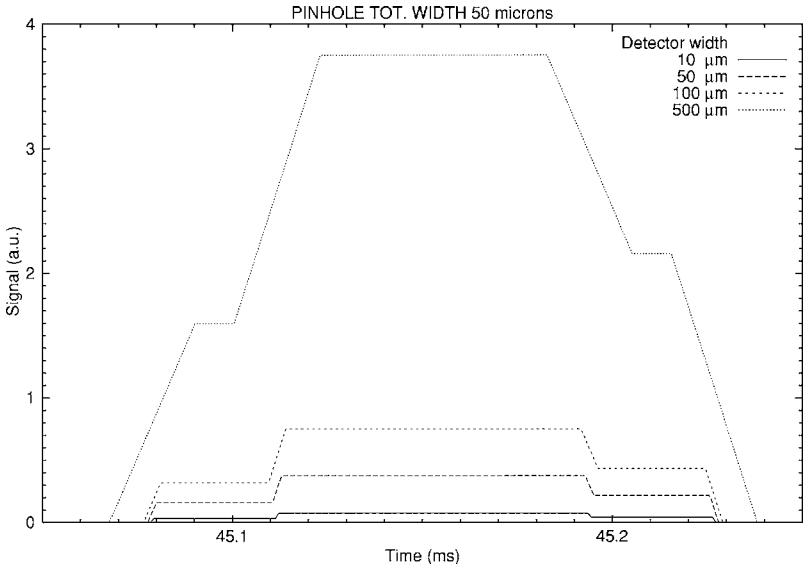

FIG. 7. Simulation of detected optical signal as a 10 μm radius droplet illuminated from below passes a pinhole camera configuration in which reflected light from the droplet passes through a pinhole displaced horizontally at 1 mm and 1 cm below the origin of the fall of the droplet. The detector (of various assumed widths) is at the same height and 1 cm away from the pinhole in the horizontal direction. The times between the kink discontinuities in the signals provide measures of the drop radius.

priate. (Diffractive effects associated with Mie scattering could also be used[37], but the relatively large ratio of droplet radius to wavelength would make these somewhat difficult to detect.) Weilert *et al.*[32] reported that they could observe two spots normal to the incident light direction corresponding to the two points on the droplet surface from which the beam was reflected. These spots were observed both with optical light from a helium neon laser and with infrared light (1.06 μm) from Nd:YAG laser and were shown to be at a separation of the droplet diameter divided by $\sqrt{2}$. By placing photodetectors with collimated apertures along the path of the falling droplets so that they mainly detect light normal to the direction of fall one expects to see two pulses at each detector, separated in time by $d/(\sqrt{2}v)$ where v is the droplet velocity. To explore the problems of resolving such a signal to determine the radius of the droplet we made a simulation of the optical signal from a falling droplet assuming a cylindrical profile and applying the Fresnel laws (Appendix C). (A spherical profile will give lower intensity but a similar time dependence.) We find two peaks separated by $d/(\sqrt{2})$ as reported in Ref. 32 as well as several lower intensity peaks at other angles. Taking a droplet radius of 10 microns and a detector positioned 1 cm from the top of the trajectory, we show the simulated signal for detector widths of 10, 50, 100, and 500 microns in Fig. 7. With these parameters, the signal could be used to determine the drop radius as well as serving as a marker for the time near the start of its fall. To get an idea of the resolution which might be possible in the measurement of the droplet radius, we repeated the simulations for various droplet radii and used the results to estimate that the required time resolution to distinguish an 11 micron from a 10 micron droplet. We find that, with these parameters, the required time resolution is of the order of 30 microseconds which is quite feasible. Thus it appears that a radius measurement of accuracy of the order of 10% (or better) of the droplet radius may be possible in this way for droplets of size in the 10 micron range.

IV. DISCUSSION AND CONCLUSIONS

We find that an experiment in which a droplet falls at low velocity through a vapor should experience decelerations due to encounters with the vapor which are attenuated in a measurable way by anomalous transmission processes of the sort we have postulated. In any case, these experiments will extend to measurements of energy and momentum transfer from helium atoms to droplets carried out by the Toennies group to a range of mean incident atomic energies which is lower, relative to the ground state of the droplet, by nearly an order of magnitude. (Relative to the vacuum level, the energies are smaller by more than 5 orders of magnitude. The latter consideration means that the mean wavelength of the incident particles is of the order of 100 nm, much longer than in any earlier experiment. There will be, however, a very large thermally induced spread of wavelengths down to around 1 nm around this small mean value if the ambient gas is at 1 K.)

In terms of the measurement of the inelastic fraction f_i of incident atoms (which is 1 if there is no anomalous transmission) we estimate that a determination of the deviation of f_i from 1.00 can probably be made at the 10% level using the techniques discussed around 1 K with 10 micron radius droplets. The main limitation on the experimental resolution is the measurement of the droplet radius for which we discussed an optical method which may be limited to an accuracy of around 10% for 10 μm droplets. One could probably do better than this if an optical window is available in the cryostat, permitting more sophisticated optical analysis of the separations of spots of light scattered from the falling droplets.

The measurements could obviously be extended to ^{3}He, both in the ambient vapor and in the droplet and this may provide a null result for comparison with the results on ^{4}He since no anomalous transmission is expected. (The only parameters which change in the analysis for ^{3}He are the liquid and vapor densities, which are extremely well known.)

If a finite value of $f_x=1-f_i$ is definitely detected in this experiment, then we have argued that condensate mediated transmission is present. By measurement of the temperature dependence of f_x one could then extract information about the velocity dependence of the transmission coefficient $T(v)$ (Appendix B). Though $T(v)$ depends on the condensate frac-

tion, the existing variational calculation of $T(v)$ in Ref. (15) does not give sufficient information to permit deduction of the condensate fraction, given $T(v)$. However diffusion Monte Carlo calculations, currently under way, will give better information about $T(v)$, permitting extraction of quantitative information about the condensate fraction.

ACKNOWLEDGMENTS

This work was supported by two NASA GSRP awards, by NSF Grant No. NSF/DMR 9980329, and by the Physics Department, the Graduate School, the Institute of Technology and the Supercomputing Institute of the University of Minnesota. Clayton Giese and William Zimmermann are thanked for discussions.

APPENDIX A: MASS AND ENERGY CHANGES OF THE DROPLET

In solving the equation of motion for the falling droplet, we neglected mass and temperature changes of the droplet. Within the same approximations used to write Eq. (1), we find that the mass change is

$$dM/dt = m \int\int [\hat{n}\cdot(\vec{v}-u\hat{z})]\rho(\vec{v})d\vec{v}dS - \int\int (\hat{n}\cdot\vec{v}')\rho(\vec{v}')d\vec{v}'dS$$

in the same notation. Expanding in u and evaluating the integrals we find that the leading term in the rate of change of the droplet's mass is of second order in u,

$$\frac{dM}{dt} = \frac{2}{3}m\pi R^2 u^2 \rho_g \sqrt{\frac{m}{2\pi k_B T}}.$$

For the suggested experimental parameters, this corresponds to a fractional rate of increase of the droplet's mass of about 5×10^{-6} s^{-1} which is negligible.

Similarly the rate of change of the thermal energy E of the droplet is given by

$$dE/dt = \int\int [\hat{n}\cdot(\vec{v}-u\hat{z})](mv^2/2)\rho(\vec{v})d\vec{v}dS - \int\int (\hat{n}\cdot\vec{v}')[m(\vec{v}'+u\hat{z})^2/2]\rho(\vec{v}')d\vec{v}'dS.$$

Expanding in u we find that, as for mass, the leading term is of second order,

$$\frac{dE}{dt} = -\frac{2}{3}\pi R^2 u^2 \rho_g \sqrt{\frac{2mk_BT}{\pi}}.$$

This corresponds to the droplet's temperature decreasing at the rate of approximately 10^{-4} K/s for our suggested experimental parameters. Here we have assumed that the thermal conductivity[39] $\kappa \approx 3.3\times10^{-5}$ W/cm K of the helium vapor near 1 K at the vapor pressure is large enough so that the temperature of the vapor near the droplet remains unchanged. Actually, using this value of thermal conductivity, one finds a thermal time constant for dissipation of thermal gradients on the 10 micron scale of about. 0.15 s, so that the droplet can be expected in steady state to be about 10^{-5} K above the temperature of the ambient gas during the fall. The effects of this temperature difference on the terminal velocity are much less than 1% under the postulated conditions of the experiment.

APPENDIX B: EFFECTS OF TRANSMISSION COEFFICIENT DEPENDING ON INCIDENT VELOCITY

If we take explicit account of a velocity dependent transmission coefficient then the right-hand side of Eq. (9) becomes

$$\frac{d\vec{p}}{dt} = \int\int [\hat{n}\cdot(\vec{v}-u\hat{z})](m\vec{v})[1-T(\vec{v}-\vec{u},\hat{n})]\rho(\vec{v})d\vec{v}dS - \int\int (\hat{n}\cdot\vec{v}')[m(\vec{v}'+u\hat{z})][1-T(\vec{v},\hat{n})]\rho(\vec{v}')d\vec{v}'dS + Mg\hat{z}. \tag{B1}$$

Substituting $\vec{v}\prime\prime = \vec{v}-\vec{u}$ and expanding to first order in $\vec{u}$, the two terms involving integrals on the right-hand side become

$$\vec{u}\int\int [\hat{n}\cdot\vec{v}'']m\rho(\vec{v})[1-T(\vec{v},\hat{n})]d\vec{v}dS - \vec{u}\int\int [\hat{n}\cdot\vec{v}']m\rho(\vec{v})\times[1-T(\vec{v},\hat{n})]d\vec{v}dS + \int\int [\hat{n}\cdot\vec{v}'']m\vec{v}\vec{u}\cdot\nabla_{\vec{v}''}[\rho(\vec{v})]\times[1-T(\vec{v},\hat{n})]d\vec{v}dS. \tag{B2}$$

Here the integrals on $\vec{v}''$ for fixed $\hat{n}$ are constrained to $\hat{n}\cdot\vec{v}''<0$ and the integral on v' for fixed $\hat{n}$ is constrained to $\hat{n}\cdot\vec{v}'>0$. If one takes $1-T(\vec{v})=f_i$ a constant in this then one gets Eq. (10). However taking $T(\vec{v},\hat{n})=\Sigma_l t_l(v)P_l(\hat{n}\cdot\hat{v})$ one can evaluate the integrals term by term in terms of the unknown functions $t_l(v)$. (P_l are Legendre polynomials.) Keeping only the terms $l=0,1$, which we found to give the largest transition amplitude in weak coupling calculations we find

$$-\vec{u}m\rho_g 4\pi R^2\left(2\pi\int v^3\rho(v)[1-t_0(v)]dv - (m\pi/3k_BT)\int v^5\rho[1-t_0(v)]dv - (m\pi/9k_BT)\int v^5\rho(v)t_1(v)dv + \cdots\right) \tag{B3}$$

which is the same as the friction term in (10) if

$$f_i = \frac{3[\cdots]}{2\pi\int \rho v^3 dv} \tag{B4}$$

in which $[\cdots]$ is the expression in square brackets in the preceding equation. This reduces to 1 if $T=0$ and to $1-t_0$ if T is independent of velocity. However for more realistic ve-

locity dependences, f_i will have a temperature dependence arising from the temperature dependence of the Maxwell velocity distribution $\rho(v)$. The resulting temperature dependence of f_i will then depend on the v dependence of the functions $t_l(v)$ [though the $t_l(v)$ themselves do not depend on temperature].

APPENDIX C: SIMULATION OF OPTICAL SIGNAL FROM A DROPLET

In order to illustrate detection of the droplet, we performed numerical simulations utilizing geometrical optics. For simplicity, we considered scattering of light from a cylinder, with light polarization along the cylinder's axis. The surface was assumed to be uniformly lit.

The simulation involved summing the intensities produced by the light beams incoming at distributed locations on the surface. Each incoming beam produced series of exit beams due to numerous internal reflections of which only the directly reflected and first internally reflected beams turn out to be significant. The intensity of each beam is determined by applying Fresnel relations for the transmission and reflection coefficients T and R,

$$T_{n\to n'} = \left(\frac{2n\cos\alpha}{\sqrt{n'^2 - n^2\sin^2\alpha} + n\cos\alpha} \right)^2,$$

$$R_{n\to n'} = \left(\frac{\sqrt{n'^2 - n^2\sin^2\alpha} - n\cos\alpha}{\sqrt{n'^2 - n^2\sin^2\alpha} + n\cos\alpha} \right)^2,$$

where α is the angle of incidence of light from media with index of refraction n into media with index of refraction n'.

We assumed a pinhole camera configuration for detection, allowing reflected light to pass from the droplet to a detector. A mask containing a slit is assumed to be placed parallel to the direction of fall. The slit is assumed to be near the position of the origin of the fall so that the droplet will be moving slowly to maximize resolution in a measurement of the time dependence of the detected intensity. To maximize magnification, we assumed that the slit was close to the trajectory (we took 1 mm for that distance) and that the detector was placed at the same height and at a larger distance (we took 1 cm) horizontally away from the slit. The magnification is the ratio of the distance from the slit to the detector, taken to be 1 cm, to the distance from the droplet to the slit which we take to be 1 mm. The resolution is controlled by the slit width which must be large enough to avoid diffractive smearing as familiar in telescope design, and to a more limited extent by the width of the detector. Intensity will be reduced for smaller slit widths. The simulation results shown used a 50 μm slit width. The droplet was assumed to be in free fall, $x=h-gt^2/2$, where $h=1$ cm is the distance from the slit center to the position at which the drop originates. We show a characteristic simulated signal in Fig. 7. The steps on the right-hand and left-hand sides of the signals permit a measurement of the droplet size. At the leading edge of the signal only the directly reflected signal (earliest time) is detected, then both that signal and the first internally reflected signal are detected and in the last part of the signal, only the internally reflected light is detected. The intensity of the internally reflected beam is $T_{1\to n}R_{n\to 1}T_{n\to 1}$. The distance between the intensity peaks in these two reflections is equal to $\sqrt{2}r$ where r is the droplet radius chosen for the simulation. These are presumably the two bright spots reported in Ref. 32.

[1] M. H. Anderson, J. R. Ensher, M. R. Andrews, C. E. Weiman, and E. Cornell, Science **269**, 198 (1995).
[2] C. C. Bradley, C. A. Sackett, J. J. Tollett, and R. G. Hulet, Phys. Rev. Lett. **75**, 1687 (1995).
[3] K. B. Davis, M.-O. Mewes, M. R. Andrews, N. J. van Druten, D. S. Durfee, D. M. Kurn, and W. Ketterle, Phys. Rev. Lett. **75**, 3969 (1995).
[4] F. London, Nature (London) **141**, 642 (1938).
[5] P. C. Hohenberg and P. M. Platzmann, Phys. Rev. **152**, 198 (1966).
[6] P. E. Sokol and W. M. Snow, in *Excitations in Two Dimensional and Three Dimensional Quantum Fluids*, edited by A. G. F. Wyatt and H. J. Lauter (Plenum, New York, 1991), p. 47.
[7] J. W. Halley, C. E. Campbell, C. F. Giese, and K. Goetz, Phys. Rev. Lett. **71**, 2429 (1993).
[8] J. W. Halley, Physica B **197**, 175 (1994).
[9] J. W. Halley, J. Low Temp. Phys. **93**, 893 (1993).
[10] C. N. Yang, Rev. Mod. Phys. **34**, 694 (1962).
[11] O. Penrose, Philos. Mag. **42**, 1373 (1951).
[12] O. Penrose and L. Onsager, Phys. Rev. **104**, 576 (1956).
[13] A. Wynveen, A. Setty, A. Howard, J. W. Halley, and C. E. Campbell, Phys. Rev. A **62**, 023602 (2000).
[14] U. V. Poulsen and K. Molmer, Phys. Rev. A **67**, 013610 (2003).
[15] A. K. Setty, J. W. Halley, and C. E. Campbell, Phys. Rev. Lett. **79**, 3930 (1997).
[16] C. D. H. Williams and A. F. G. Wyatt, Phys. Rev. Lett. **91**, 085301 (2003).
[17] K. A. Lidke, A. Wynveen, N. Baisch, C. Koay, C. F. Giese, and J. W. Halley, J. Low Temp. Phys. **140**, 429 (2005).
[18] J. Harms and J. P. Toennies, Phys. Rev. Lett. **83**, 344 (1999).
[19] M. A. Weilert, D. L. Whitaker, H. J. Maris, and G. M. Seidel, Phys. Rev. Lett. **77**, 4840 (1996).
[20] E. Krotscheck and R. Zillich, J. Chem. Phys. **115**, 10161 (2001).
[21] M. A. H. Tucker and A. F. G. Wyatt, J. Low Temp. Phys. **110**, 425 (1998).
[22] M. A. H. Tucker and A. F. G. Wyatt, J. Phys.: Condens. Matter **4**, 7745 (1992).
[23] A. F. G. Wyatt, J. Low Temp. Phys. **87**, 453 (1992).
[24] E. Farhi, B. Fak, C. M. E. Zeyen, and J. Kulda, Physica B **297**, 32 (2001).
[25] K. R. Atkins, *Liquid Helium* (Cambridge University Press, Cambridge, 1959).
[26] L. D. Landau and I. M. Khalatnikov, Zh. Eksp. Teor. Fiz. **19**, 637 (1949); **19**, 709 (1949), Ref. 25.

[27] P. Roche, M. Roger, and F. I. B. Williams, 1Phys. Rev. B **53**, 2225 (1996).
[28] P. Roche, G. Deville, K. O. Keshishev, N. J. Appleyard, and F. I. B. Williams, Phys. Rev. Lett. **75**, 3316 (1995).
[29] R. J. Donnelly and C. F. Barenghi, J. Phys. Chem. Ref. Data **27**, 1217 (1998).
[30] J. A. Northby, J. Chem. Phys. **115**, 10065 (2001).
[31] H. Kim, K. Seo, B. Tabbert, and G. A. Williams, J. Low Temp. Phys. **121**, 621 (2000).
[32] A. Weilert, D. L. Whitaker, H. J. Maris, and G. M. Seidel, J. Low Temp. Phys. **98**, 17 (1995).
[33] G. A. Williams (private communication).
[34] J. Wilks, *The Properties of Liquid and Solid Helium* (Clarendon, Oxoford, 1967), p. 415.
[35] J. J. Niemela, J. Low Temp. Phys. **109**, 709 (1997).
[36] B. Bennett, A. Shumays, L. C. Krysac, and J. D. Maynard, J. Low Temp. Phys. **113**, 1073 (1998).
[37] I. Weiner, M. Rust, and T. D. Donnelly, Am. J. Phys. **69**, 129 (2001).
[38] J. Butterworth *et al.*, Rev. Sci. Instrum. **69**, 3697 (1998).
[39] K. Fokkens, K. W. Taconis, and R. de Bruyn Ouboter, in *Proceedings of the Eighth International Conference on Low Temperature Physics*, edited by R. O. Davies (Butterworths, Washington, 1963), pp. 34–36.